

Physico-chemical Properties of Nb/Ti Binary Oxides and their Photo-catalytic Activities

Shi-Jane Tsai (蔡世貞) and Soofin Cheng* (鄭淑芬)

Department of Chemistry, National Taiwan University, Taipei, Taiwan 106, R.O.C.

A series of binary Nb/Ti oxides was prepared by co-precipitation. Their structure and physico-chemical properties in terms of surface area, surface acidity, bandgap energy and life time of the radiation-excited electron-hole pair were examined. These properties were correlated to their catalytic activities in photo-degradation of oxygenated or organic pollutants in water. The organic pollutants under investigation were phenol, cyclohexanol and tetrahydrofuran (THF). The lab-made titanium oxide and those doped with a small amount of Nb (molar ratio of Nb/(Nb+Ti) less than 20%) showed higher activities in degradation of the organic pollutants. However, the mineralization efficiencies were different for the three oxygenated or organic pollutants. Nearly complete mineralization to form CO₂ could be achieved in the degradation of phenol. For cyclohexanol, only ca. 50% selectivity of CO₂ was obtained over all the catalysts. Similar low efficiency in complete mineralization was observed in the degradation of THF, but higher selectivity (ca. 65-75%) of CO₂ could be obtained on the binary oxide with Nb content less than 4 mol %. In contrast, the binary Nb/Ti oxide with equal Nb and Ti molar content gave the poorest catalytic activity. The photocatalytic activity is generally correlated well to the life time of the radiation-excited electron-hole pairs. The contribution of surface acidity to the photocatalytic activity was only demonstrated on the niobia-dominant oxide catalysts toward THF. The photocatalytic activity was found to have no correlation with the crystal structure, the bandgap energy, the surface area or the surface hydroxyl density.

INTRODUCTION

Research in the photo-degradation of the harmful organic pollutants in waste water by semiconductor materials has been growing steadily over the last decade.¹ Titanium oxide is an n-type semiconductor and a typical photocatalyst. The advantage of utilization of titanium oxide in the composition of organic pollutants includes its low cost, radiation stability, and no need of using strong oxidizing agents, such as O₃ or H₂O₂.²

Many factors were considered to influence the photocatalytic activity of TiO₂, such as the crystal structure, particle size, bandgap energy, acidity and density of hydroxyl groups on the catalyst surfaces. However, the effect of these factors is still controversial. For instance, anatase is commonly found more active than rutile in photocatalysis.³⁻⁵ Nevertheless, several studies showed that the activity was more influenced by the preparation method of the catalyst.⁶⁻⁷ Surface acidity is another important factor commonly discussed. Studies on the acidity of either anatase or rutile by pyridine adsorption have demonstrated that the surface acidity is mainly of the Lewis type.⁸⁻¹¹ The commercial Degussa

P-25 TiO₂, which has been the most frequently studied photocatalyst, contains 70% anatase and 30% rutile. The catalytic activity of Degussa P-25 TiO₂ in the photodegradation of 1,4-dichlorobenzene was reported to improve by impregnating a suitable amount of MoO₃, WO₃,¹² or Nb₂O₅.¹³ In these cases, surface acidity was proposed to be the important factor affecting the efficiency of the catalysts. Binary oxides prepared by mixing other metal ions into TiO₂ through the co-precipitation method are more commonly studied. The effect of the second metal species on photocatalytic activities of the binary oxides however is quite varied. More enhanced photocatalytic activities in degradation of organic pollutants than on pure TiO₂ were reported on TiO₂ doped with a small amount of transition metal or lanthanide ions,¹⁴⁻¹⁶ but lower activities were observed on Cr(III) and Ce(IV) doped TiO₂.^{17,18} Mixed metal oxides often generate additional acid sites, especially Bronsted acid type. In several of these studies, the surface acidity was thought to contribute surface hydroxyl groups, which play an important role in stabilizing holes generated by illumination and oxidizing adsorbed molecules.^{6,7} On the other hand, improved photocatalytic activities in decomposition of organic species were reported on TiO₂/SiO₂

Dedicated to Professor Sheng-lieh Liu on the occasion of his ninth birthday.

* Corresponding author. Fax: +886-2-23636359; E-mail: chem1031@ccms.ntu.edu.tw

and $\text{TiO}_2/\text{Al}_2\text{O}_3^{19,20}$ and $\text{TiO}_2/\text{molecular sieves}^{21}$. The second metal oxide was considered to facilitate the adsorption of the organic substrates and make them more easily approach the active TiO_2 sites.

Niobium oxide and niobium compounds are interesting for their activities in catalysis. Hydrated niobium oxide was reported to have strong acidity and exhibit high activity in acid-catalyzed reactions.²² Niobia, when used as a support, was reported to promote reactivity of platinum catalysts.^{23,24} The effects were associated with the strong metal-support interaction, which was the phenomenon first observed on noble metals supported on TiO_2 .²⁵ Besides, layered niobates demonstrated high activities in photo-decomposition of water and alcohols.²⁶⁻²⁸ However, the photocatalytic activity of niobium oxide in degradation of organic pollutants has received little attention. In this study, a series of binary Nb/Ti oxides was prepared. Their activities in the photo-degradation of oxygenated organic compounds were compared in order to understand the factors which affect the photocatalytic activity.

EXPERIMENTAL METHODS

Catalyst Preparation

Reagent grade chemicals were used as purchased without further purification. NbOCl_3 solution was prepared by dissolving NbCl_5 (Janssen) in concentrated HCl (Janssen), followed by dilution to make 0.1 M solution. TiOCl_2 solution was prepared by mixing an equal weight of TiCl_4 (Merck) and 1.0 M HCl solution. The binary oxides of different Nb/Ti molar ratios were prepared by refluxing the stoichiometric mixture of TiOCl_2 and NbOCl_3 solutions for 3 h. The resultant

solids were filtered, washed with doubly deionized water until free of Cl^- ions, and followed by drying at ambient temperature. The catalysts were named as NTs, where "s" represents Nb/(Nb+Ti) molar ratio in percentage.

Characterization Techniques

BET surface area was determined by physical adsorption of N_2 at liquid N_2 temperature in a volumetric system. The powder XRD patterns were examined with a Scintag X1 diffractometer using Cu K α radiation. The FT-Raman spectra were recorded using a BOMEM MB155 IR/Raman spectrometer with a Nd-YAG laser (1064 nm) source. Diffuse reflectance UV-Vis spectra of powder samples were obtained with a Shimadzu UV-2101PC spectrometer. The bandgap energies of the catalysts were determined based on the absorption threshold of their UV-Vis spectra. The lifetime of radiation-excited electron-hole pairs was monitored by examining the luminescence life time of the solid catalysts with a time-resolved spectrometer, in which 355 nm light source generated from a Nd-YAG laser was used and detection was set at 450 nm. The surface hydroxyl groups of powder samples were examined using a BOMEM MB155 IR spectrometer equipped with a Harrick diffuse reflectance cell. The acidity of the catalysts was determined by temperature programmed desorption (TPD) of NH_3 using a DuPont 951 TGA system.

Photocatalytic Activities

A Rayonet photochemical chamber reactor of model no. PRP-100 was used for photocatalysis study. Detailed setup of the apparatus was described previously.⁷ The catalyst in powder form based on the same metal equivalence as 0.01 g TiO_2 (amount listed in Table 1), was suspended in a 50

Table 1. Phase Composition, Surface Area and the Weight Used in Photocatalysis of Nb/Ti Binary Oxides

Catalyst	Nb/(Nb+Ti) (%)	S. A. (m^2g^{-1})	Phase composition ^a (%)		Catal. wt ^b (g)
			Anatase	Rutile	
LR	0	141	0	100	0.0100
NT01	1	81	9	91	0.0100
NT04	4	105	20	80	0.0103
NT07	7	190	58	42	0.0105
NT11	11	190	64	36	0.0110
NT19	19	149	77	23	0.0113
NT50	50	228	88	12	0.0133
NT95	95	301	- ^c	-	0.0163
NT100	100	300	-	-	0.0166

^a Determined by XRD patterns.

^b The same metal equivalence as 0.01 g TiO_2 .

^c Amorphous phase.

mL aqueous solution of 1.25 mM oxygenterminated organic compound. The organic substrates under investigation included phenol, cyclohexanol and tetrahydrofuran. O₂ gas of 10 mL/min was bubbled through as oxidant, and 300 nm UV radiation was the light source. The outlet gases were directed through a two-stage bubbling trap containing saturated Ba(OH)₂ solution, and the CO₂ yield was determined based on the weight of BaCO₃ precipitated. Gas products were analyzed off-line during the reaction course. The liquid products retained in aqueous solution after 6 h radiation were separated with a Hewlett Packard 5890 GC using a Rtx-5 capillary column of 60 m length and detected by a FID detector.

RESULTS

Structure characterization

The crystalline structure of the Nb/Ti binary oxides was identified by x-ray diffraction (Fig. 1). Rutile was the crystalline phase observed on pure titanium oxide, and the sample was termed LR (abbreviation for lab-made rutile). As Nb of as low as 1% was doped into the oxide, some anatase phase appeared. Based on the area ratio of the peak at $2\theta = 25.3^\circ$ for anatase to that at 27.4° for rutile, the composition of the crys-

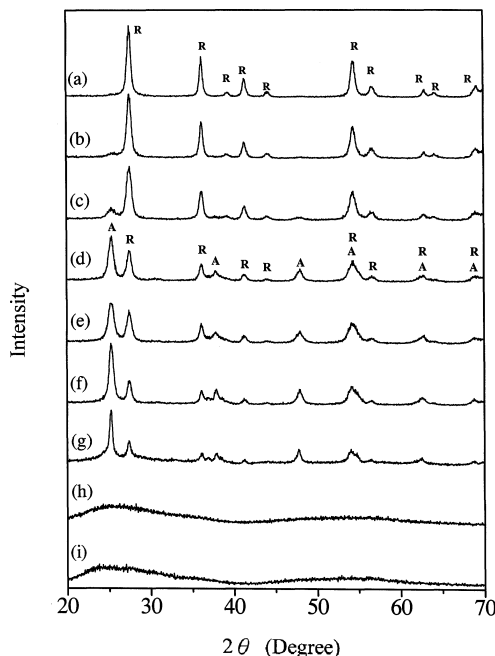


Fig. 1. XRD patterns of as-prepared Nb/Ti binary oxides, (a) LR, (b) NT01, (c) NT04, (d) NT07, (e) NT11, (f) NT19, (g) NT50, (h) NT95 and (i) NT100; where A: anatase and R: rutile.

talline phases in the binary oxides was determined and the results are tabulated in Table 1. The amount of the anatase phase increased with the Nb content. When niobium oxide became dominant, such as Nb/(Nb+Ti) molar ratio $\geq 95\%$, the solids turned to amorphous.

The Raman spectra of the samples with low Nb content showed two peaks at 603 and 437 cm⁻¹ (Fig. 2), which are the characteristic Ti-O vibrational peaks of rutile.²⁹ These two peaks shift toward 616 and 434 cm⁻¹, respectively, as Nb was added into the oxide. When the Nb content is increased to Nb/(Nb+Ti) $\geq 11\%$, two additional peaks appear at 514 and 280 cm⁻¹. The 280 cm⁻¹ peak grows with the increase of Nb content, while the 514 cm⁻¹ peak disappears. For the binary oxides of amorphous structure (NT95 and NT100), two very broad peaks appear at 636 and 280 cm⁻¹, which correspond to the vibrational modes of NbO₆ octahedra and Nb-O-Nb linkage, respectively.³⁰ The three characteristic vibrational peaks of anatase TiO₂, which should appear at 640, 515 and 395 cm⁻¹,²⁹ were not observed in the Raman spectra of the binary oxides. These results infer that the anatase structure observed in XRD patterns is not due to pure TiO₂ structure. Instead, it

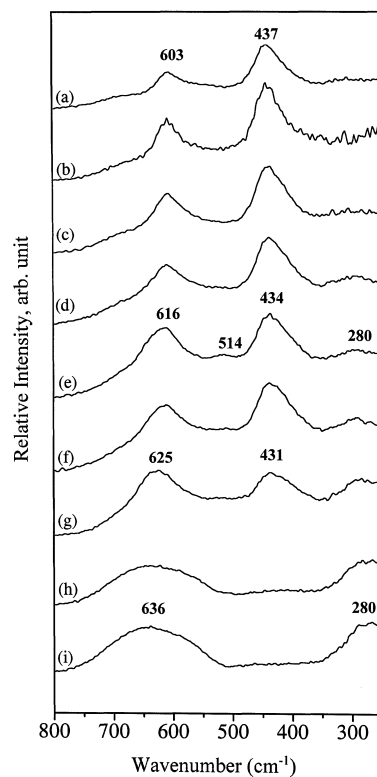


Fig. 2. Raman spectra of as-prepared Nb/Ti binary oxides, (a) LR, (b) NT01, (c) NT04, (d) NT07, (e) NT11, (f) NT19, (g) NT50, (h) NT95 and (i) NT100.

should be an oxide of Nb and Ti mixed in the molecular level. Rutile is the densest phase of TiO_2 and thermodynamically most stable in comparison to other phases. The formation of anatase phase instead of rutile in Nb/Ti binary oxides is attributed to the perturbation of crystal growth when Nb(V) ions of relatively larger size and with excess positive charge than Ti(IV) were incorporated into the oxide structure. A similar phenomenon was also observed on the growth process of nanosize rutile, where the crystalline phase was greatly influenced by the addition of NH_4Cl as mineralizer.³¹

Fig. 3 shows that all samples have absorption in the O-H stretching vibration region. The as-prepared samples show broad absorption bands covering 2500–3750 cm^{-1} region, demonstrating the presence of H-bonding among the O-H groups and the physically-adsorbed water molecules. The intensity of the broad bands was markedly reduced and discrete peaks appeared after the samples were evacuated at 400 °C. Lab-made TiO_2 has the peak maximum appearing at 3670 cm^{-1} , lab-made Nb_2O_5 at 3686 cm^{-1} , and the binary oxides show a combination of both peaks in different intensity ratios.

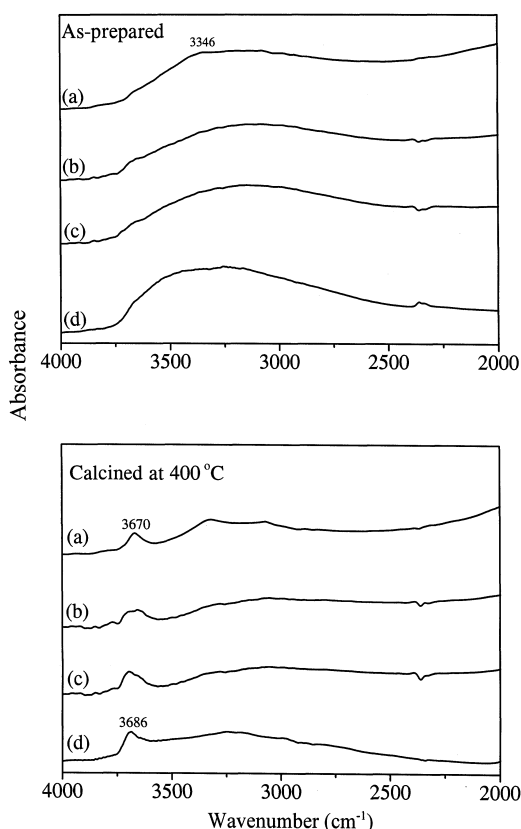


Fig. 3. Diffuse reflectance IR spectra in the O-H stretching region of as-prepared and calcined Nb/Ti binary oxides, (a) LR, (b) NT11, (c) NT50 and (d) NT100.

Other physico-chemical properties

The physico-chemical properties of various Nb contents in term of surface area, surface acidity, bandgap energy and lifetime of the radiation-excited electron-hole pair are summarized in Fig. 4. The binary oxides except those with amorphous structure have similar bandgap energies as that of lab-made rutile TiO_2 (LR), while the niobia dominant samples NT95 and NT100 show an apparent blue shift relative to either lab-made rutile (3.04 eV) or commercial Nb_2O_5 (2.86 eV). These two amorphous oxides consistently have the highest BET surface area and surface acidity. Since the higher the surface area, the smaller the particle sizes, the blue shift of the bandgap energies is likely a result of the particle size quantization effect.³² Fig. 4 also shows that the acid amounts are similar for the binary oxides of Nb contents smaller than 50%, while the BET surface area generally increases with Nb content. Both values however reach the maximum for niobia-dominant samples. On the other hand, the luminescence life time has little correlation

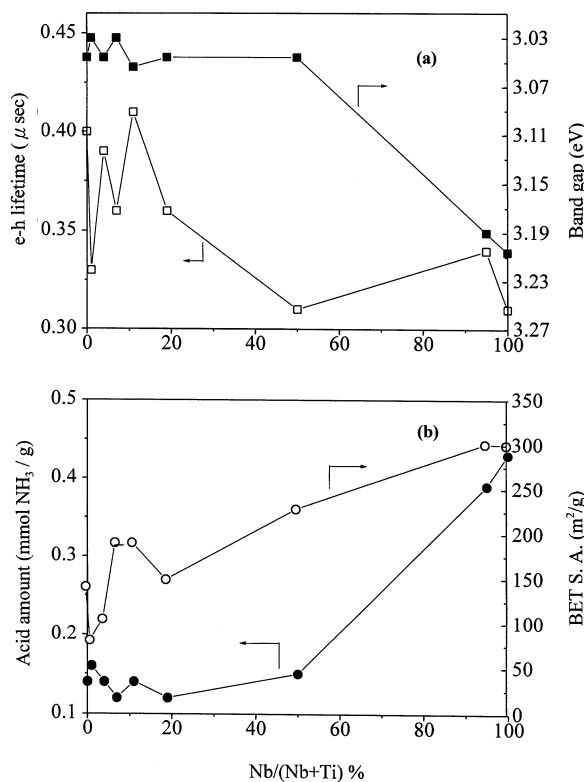


Fig. 4. Physico-chemical properties of Nb/Ti binary oxides as a function of Nb content, (a) luminescence life time and bandgap (b) acid amount and BET surface area.

with the Nb content. The inversion of the life time is proportional to the electron-hole recombination rate. The results oppose the proposal that larger bandgap energy generally has lower recombination rate.³³ The longest life times were observed on lab-made rutile TiO₂, as well as the binary oxides containing 4 and 11% Nb, while the shortest life times were found on pure Nb₂O₅ and NT50.

Photocatalytic activities of TiO₂ of different crystalline phases

The results of photo-decomposition of oxygenated organic substrates in aqueous solutions over lab-made-rutile (LR) were compared with those over commercial TiO₂ and tabulated in Table 2. Although the commercial anatase TiO₂ shows the highest conversions based on the disappearance of the organic substrates, its efficiencies in complete mineralization to form CO₂ are rather low. The mineralization efficiency was also found to vary with the organic substrate. It decreases from 55.4, 34.1 to 14.2% for phenol, THF and cyclohexanol, respectively. On the other hand, the commercial rutile TiO₂ shows very low activities in degradation, which is consistent with most of the literature results. On the contrary, lab-made rutile gave relatively high conversions and mineralization efficiencies. Moreover, it is much more efficient than the commercial anatase in complete oxidation of the organic substrates to CO₂. These results demonstrate

that the crystalline phase is not a key factor in determining the catalytic activity of photodegradation.

In order to examine the effect of catalyst surface area, photo-degradation of phenol was carried out with lab-made rutile calcined at different temperatures but based on a catalyst amount of the same total surface area. Table 3 shows that both the conversion and the mineralization efficiency decrease with the calcination temperature of rutile. The results rule out that the catalytic activity is proportional to the surface area. Instead, the number of surface hydroxyl groups is probably more important.

Photocatalytic activities of the Nb/Ti binary oxides

Fig. 5 shows the photo-degradation rates of the three organic substrates over the Nb/Ti binary oxides of various Nb contents. The highest conversion and mineralization efficiency were observed over the binary oxides with Nb content lower than 11%, while the minimum activities were observed over the binary oxides with Nb/Ti molar ratio higher than 1. The maximum activity however varied with different organic substrates. Based on the disappearance of organic reactant, the highest activities for the three substrates are: lab-made rutile for phenol, NT07 for cyclohexanol, and NT01 for THF. On the other hand, the highest mineralization efficiencies are: NT11 for phenol, lab-made rutile for cyclohexanol, and NT01 for THF.

Table 2. Photodegradation of the Oxygenated Organic Substrates over Various TiO₂ Catalysts

Catalyst	Organic substrate	Conv. (%)	CO ₂ Yield (%)	Miner. Eff. ^a (%)
Anatase (Commer.)	Phenol	100	55.4	55.4
	Cyclohexanol	98.6	14.0	14.2
	THF	70.0	23.9	34.1
Rutile (Commer.)	Phenol	56.5	20.5	36.3
	Cyclohexanol	40.0	2.4	6.0
	THF	37.3	13.1	35.1
LR (Lab-made rutile)	Phenol	87.9	75.4	85.8
	Cyclohexanol	72.7	38.4	52.8
	THF	73.4	55.0	74.9

^a Miner. Eff. = mineralization efficiency.

Table 3. Photodegradation of 1.25 mM Phenol over Lab-made Rutile TiO₂ Based on the Same Surface Area

Calc. Temp. (°C)	S.A. (m ² /g)	Catal. Wt. (g)	Conv. (%)	CO ₂ Yield (%)	Miner. Eff. (%)
25	141	0.0100	87.9	75.4	85.8
400	74	0.0191	83.6	63.0	75.4
700	23	0.0613	63.3	42.2	66.7

DISCUSSION

Effect of the organic substrates

The interaction of the organic substrates with the surface generated·OH radicals was considered to be the primary step of the photo-degradation in aqueous solutions.^{2,34} Phenol is the most electrophilic among the three organic substrates. Over TiO₂ catalysts of different crystalline phases, the conversions of phenol in photo-degradation are always higher than those of THF and cyclohexanol. However, that changed on the binary oxides. For the binary oxides of low Nb content, phenol is no longer the one achieving the highest conversion. Over several catalysts, the conversions of cyclohexanol are over that of phenol. The dielectric constants of these three compounds decrease in the order of cyclohexanol ($\epsilon = 16.4$) > phenol ($\epsilon = 12.4$) > THF ($\epsilon = 7.5$). Since there are hydroxyl

groups on the catalyst surface, the high affinity of cyclohexanol to the catalyst surface may account for the high conversion of cyclohexanol.

For niobia dominant oxides, THF has higher conversions than the other two organic substrates. Therefore, there must be factors other than electrophilicity and dielectric constant of the organic substrates which influence the photo-degradation activity. Besides, the mineralization efficiencies of phenol are very high over the binary oxides with Nb content less than 11%. The efficiency decreases as the Nb content increases. It is also noticed that over the binary oxides of low Nb contents the mineralization efficiencies of cyclohexanol are the lowest among the organic substrates. Therefore, cyclohexanol should generate stable intermediates which are volatile or difficult to decompose, such as cyclohexanone.

Factors on the catalysts affecting the photocatalytic activity

The Nb/Ti binary oxides of low Nb contents show higher photocatalytic activities than those of niobia dominance. The minimum activities were observed over catalyst NT50 containing equal equivalents of Nb and Ti. Lab-made TiO₂, which has rutile structure, is among the oxides of highest activities, while NT50, which contains 88% anatase and 12% rutile phase, has lowest activity. The results are contrary to those observed on the commercial anatase and rutile TiO₂. It demonstrates that the crystalline phase of the semiconductor plays little role on photocatalytic activity. Instead, the preparation method is more important in obtaining the catalysts of high photoactivity.

Effect of surface hydroxyl groups

Sclafani et al.⁶ attributed the high photoactivity of lab-made TiO₂ to surface hydroxyl groups, which were considered to trap the holes in the valence band and enhance the chemisorption of oxygen molecules in the conduction band. In the present system, FT-IR study shows no significant differences in the amount of surface hydroxyl groups among the Nb/Ti binary oxides of different Nb contents. Therefore, surface hydroxyl groups are probably not the key factor responsible for the differences in photocatalytic activities of the binary oxides.

Effect of bandgap, surface area and hot-electron life time

In comparison to the physico-chemical properties of the binary oxides shown in Fig. 4, the photocatalytic activities were found in rather good agreement with the hot-electron life time. Remarkably, the minimum on the activity profiles are consistent with those of luminescence life time. All

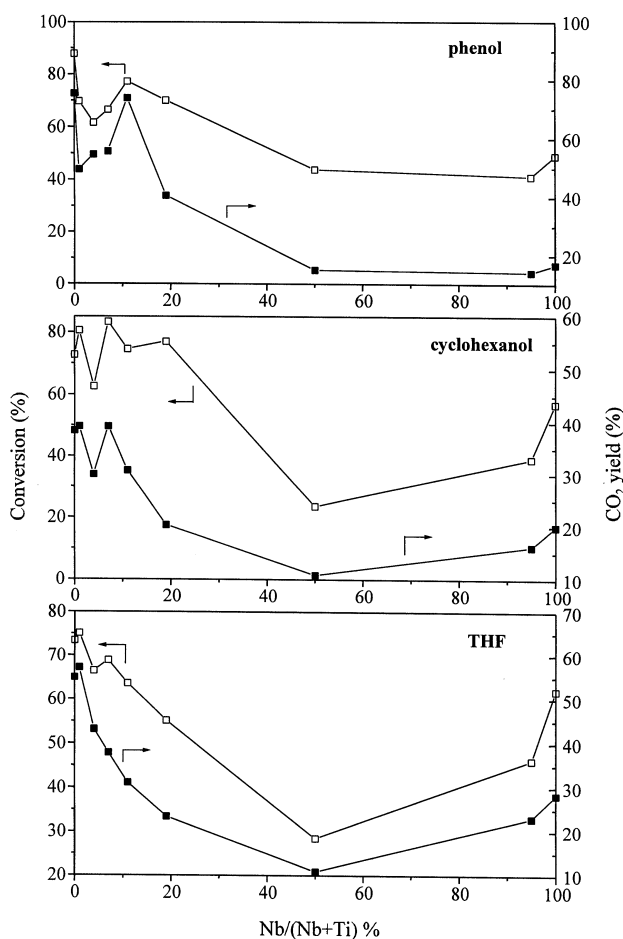


Fig. 5. Activities of photo-degradation of phenol, cyclohexanol, and THF over Nb/Ti binary oxides of various Nb contents: (○) conversion, (△) CO₂ yield, and (■) mineralization efficiency.

correspond to catalyst NT50, the binary oxide with equal equivalents of Nb and Ti. The photocatalytic activity on the other hand has little to do with the bandgap energy, since both binary oxides of the highest and lowest photocatalytic activities have similar bandgap energies. Besides, the photocatalytic activity does not increase with the surface area or the acid amount. However, that pure Nb_2O_5 is more active in degradation of all three organic substrates than NT95 is contrary to the variation of the luminescence life time. Hence, there must be factors other than the hot-electron life time that affect the photocatalytic activity. Since both niobia dominant samples have similar surface areas but NT100 has greater surface acidity than NT95, surface acidity should contribute to some extent to the photocatalytic performance.

Effect of structural defects

Another factor been brought to consideration recently is the structural defects. Sclafani and Herrmann³⁵ reported that the structural defects on the surface could photoadsorb oxygen and form O^- and O^{2-} species. In aqueous solutions, these species are considered to react with surface adsorbed water molecules to generate $\cdot\text{OH}$ radicals. Based on the bandwidths at half-maximum of the x-ray diffraction peaks in Fig. 1, the NT50 sample, which gives the lowest catalytic activities, consistently has the highest crystallinity among the binary oxides. On the other hand, the binary oxides of low Nb contents have broad diffraction peaks, indicating relatively low crystallinity, while the niobia dominant oxides have amorphous structure. According to the proposal by Sclafani and Herrmann,³⁵ the structural defects increase the oxygen-exchange ability of TiO_2 . The adsorbed oxygen reacts with the hot electrons to form O^- and O^{2-} species and that further converts to $\cdot\text{OH}$ radicals. In the present study, the structural defects are considered important in influencing the lifetime of the hot electrons and consequently the photocatalytic activity.

Effect of acidity

The importance of acidity on photocatalytic activity is demonstrated by the trend of the degradation rates of the three organic substrates. The enhancement of photoactivity by surface acidity was most obvious over the niobia dominant samples NT95 and NT100, which have greatest surface acidity among the binary oxides. In comparison of the activity profiles of the three organic substrates shown in Fig. 5, the extent of enhancement decreases in the order of THF > cyclohexanol > phenol. Surface acidity is reported to improve the photo-catalytic activity by facilitating the adsorption of basic substrates to the catalyst surface.²⁰ The interaction should be

weak for phenol since it is itself an acidic compound. Besides, acid is usually considered a catalyst in breaking bonds of ethers. Hence, the enhancement of the photo-degradation activity by acidity is most obvious for THF and least for phenol.

Moreover, both niobia-dominant catalysts were found to give serious coking during the photodegradation reactions. Hence, the acidity probably also stabilizes coke products formed on the surface. The coverage of catalyst surface with dark coke would reduce the quantum yield and lower the mineralization efficiency. As a result, the mineralization efficiencies over the niobia-dominant oxides are generally lower than those over the titania-dominant oxides.

CONCLUSIONS

We demonstrated that the crystalline structures of lab-made Nb/Ti binary oxides vary with the niobium content, from rutile, a mixture of rutile and anatase, to amorphous compounds. The bandgap energies of the binary oxides remain constant for Nb content up to 50 mol %. Particle size quantization effect was demonstrated on the variation of the bandgap energy. The bandgap energies are lowest but the surface areas and acid amount are greatest for niobia-dominant oxides. However, the photocatalytic activity was found to have little to do with the crystal line structure, the bandgap, the surface area and surface hydroxyl density. The highest conversion and mineralization efficiency in photodegradation of the three oxygenated organic substrates were observed over lab-made rutile and the binary oxides with Nb/(Nb+Ti) molar ratio less than 11%. The photocatalytic activities of the binary oxides as a function of Nb content in degradation of the three oxygenated organic substrates under investigation varied in similar patterns. The minimum was observed over the binary oxide with 1:1 Nb/Ti molar ratio. The maximum activities however vary with different organic substrates: lab-made rutile for phenol, NT07 for cyclohexanol, and NT01 for THF. The structural defects on the oxides are considered more important than other factors in stabilizing the life time of the hot electrons and increasing the photocatalytic activities. Besides, surface acidity may also enhance the degradation of the organic substrates. For the three oxygenated organic substrates under investigation, phenol is most easily degraded over TiO_2 catalysts. As the influence of acidity increases over niobia-dominant oxide, THF has higher conversion than cyclohexanol and phenol. However, a large number of acidic sites on the catalyst surface also reduces the mineralization efficiency due to serious coking on the surface.

ACKNOWLEDGMENT

Financial support from the National Science Council, Taiwan, is gratefully acknowledged.

Received September 3, 2001.

Key Words

Nb/Ti binary oxides; Catalytic; Photo-degradation; Organic pollutants.

REFERENCES

- Hoffmann, M. R.; Martin, S. T.; Choi, W.; Bahnemann, D. W. *Chem. Rev.* **1995**, *95*, 69.
- Braun, A. In *Photochemical Conversion and Storage of Solar Energy*; Pelizzetti, E.; Schiavello, M., Eds.; Kluwer, Dordrecht, 1991; p 551.
- Fox, M. A.; Dulay, M. T. *Chem. Rev.* **1993**, *93*, 341.
- Nishimoto, S.-I.; Ohtani, B.; Kajiwara, H.; Kagiya, T. *J. Chem. Soc., Faraday Trans. I* **1985**, *81*, 61.
- Tanaka, K.; Hisanaga, T.; Rivera, A. P. In *Photocatalytic Purification and Treatment of Water and Air*; Ollis, D. F.; Al-Ekabi, H., Eds.; Elsevier: Amsterdam, 1993, p 169.
- Sclafani, A.; Palmisana, L.; Schiavollo, M. *J. Phys. Chem.* **1990**, *94*, 829.
- Tsai, S.-J.; Cheng, S. *Catal. Today* **1997**, *33*, 227.
- Morterra, C. J. *Chem. Soc., Faraday Trans. I* **1988**, *84*, 1617.
- Primmet, M.; Pichaat, P.; Mathieu, M. V. *J. Phys. Chem.* **1971**, *75*, 1221.
- Miyata, H.; Nakagawa, Y.; Ono, T.; Kubokawa, Y. *J. Chem. Soc., Faraday Trans. I* **1983**, *79*, 2343.
- Kiselev, A. V.; Uvarov, A. V. *Surf. Sci.* **1967**, 399.
- Papp, J.; Soled, S.; Dwight, K.; Wold, A. *Chem. Mater.* **1994**, *6*, 496.
- Cui, H.; Dwight, K.; Soled, S.; Wold, A. *J. Solid State Chem.* **1995**, *115*, 187.
- Choi, W.; Termin, A.; Hoffmann, M. R. *Angew. Chem. Int. Ed. Engl.* **1994**, *33*, 1091.
- Yu, J. C.; Lin, J.; Kwok, W. M. *J. Photochem. & Photobio. A: Chem.* **1997**, *111*, 199.
- Yu, J. C.; Lin, J.; Kwok, W. M. *J. Phys. Chem. B.* **1998**, *102*, 5094.
- Lin, J.; Yu, J. C.; Lam, S. K. *J. Catal.* **1999**, *183*, 368.
- Brezova, V.; Blazkova, A.; Borosova, E.; Ceppan, M.; Fiala, R. *J. Mol. Catal. A: Chem.* **1995**, *98*, 109.
- Anderson, C.; Bard, A. J. *J. Phys. Chem.* **1995**, *99*, 9882.
- Anderson, C.; Bard, A. J. *J. Phys. Chem. B.* **1997**, *101*, 2611.
- Hsien, Y.-H.; Chang, C.-F.; Chen, Y.-H.; Cheng, S. *Appl. Catal. B* **2001**, *31*, 241.
- Tanabe, K.; Okazaki, S. *Appl. Catal. A* **1995**, *133*, 191.
- Passos, F. B.; Aranda, D. A. G.; Soares, R. R.; Schmal, M. *Catal. Today* **1998**, *43*, 3.
- Aranda, D. A. G.; Noronha, F. B.; Passos, F. B.; Schmal, M. *Appl. Catal.* **1993**, *100*, 77.
- Tauster, S. J.; Fung, S. C.; Garten, R. L. *J. Amer. Chem. Soc.* **1978**, *100*, 170.
- Domen, K.; Yoshimura, J.; Sekine, T.; Tanaka, A.; Onishi, T. *Catal. Lett.* **1990**, *4*, 339.
- Domen, K.; Ebina, Y.; Sekine, T.; Tanaka, A.; Kondo, J.; Hirose, C. *Catal. Today* **1993**, *16*, 479.
- Abe, R.; Shinohara, K.; Tanaka, A.; Hara, M.; Kondo, J. N.; Domen, K. *Chem. Mater.* **1997**, *9*, 2179.
- Busca, G.; Ramis, G.; Amores, J. M. G.; Escribano, V. S.; Piaggio, P. *J. Chem. Soc., Faraday Trans.* **1994**, *90*, 3181.
- Wachs, I. E.; Jehng, J.-M.; Hardcastle, F. D. *Solid State Ionics* **1989**, *32*, 904.
- Cheng, H.; Ma, J.; Zhao, Z.; Qi, L. *Chem. Mater.* **1995**, *7*, 663.
- Hagfeldt, A.; Gratzel, M. *Chem. Rev.* **1995**, *95*, 49.
- Nozik, A. J. In *Photocatalytic Purification and Treatment of Water and Air*; Ollis, D. F.; Al-Elabi, H., Eds.; Elsevier: Amsterdam, 1993; p 39.
- Pelizzetti, E.; Minero, C. *Electrochimica Acta* **1993**, *38*, 47.
- Sclafani, A.; Hermann, J. M. *J. Phys. Chem.* **1996**, *100*, 13655.